Journal of Innovative Optical Health Sciences
Vol. 12, No. 1 (2019) 1841001 (7 pages)

DOI: 10.1142/S1793545818410018

World Scientific
www.worldscientific.com

Force-dependent unfolding and folding dynamics of protein alpha-catenin modulation domains

Xueping Li, Weili Zhai, Zilong Guo and Hu Chen*
Research Institute for Biomimetics and Soft Matter
Fujian Provincial Key Lab for Soft Functional Materials Research
Department of Physics, Xiamen University, Xiamen, China
**chenhu@xmu.edu.cn*

Received 12 April 2018
Accepted 8 May 2018
Published 13 June 2018

α-catenin is an adhesion protein located at the cadherin-based cell–cell adherens junction. α-catenin cross-links β-catenin and actin fiber in the adhesion protein complex, and plays an important role in the formation and modulation of cell–cell adhesion. The central modulation domains can be unfolded to expose binding site of vinculin when stretching force is applied. Here, we studied the force-induced unfolding dynamics of α-catenin modulation domains under different loading rates from which the unfolding distance of M2 and M3 domains is determined to be 5–7 nm, and an unfolding intermediate state is identified. We also found that the folding process of M1–M3 domains goes through different pathways with cooperativity.

Keywords: α-catenin; folding and unfolding; magnetic tweezer; Bell's model.

1. Introduction

Adherens junction between cells plays an important role in many biological processes, such as cell morphogenesis, cancer cell metastasis, wound healing, and embryonic development.[1] In adherens junction, extracellular domain of transmembrane protein E-cadherin binds with E-cadherin on adjacent cells to link cells together, while cytoplasmic domain of E-cadherin links to actin fiber cytoskeleton through cross-linker proteins of β-catenin and α-catenin.[2]

The catenins not only function as cross-linkers, but also regulate the growth of adhesion site in a force-dependent manner.[3] β-catenin binds cytoplasmic domain of E-cadherin to form a protein complex. N-terminus of α-catenin binds β-catenin, and C-terminus of α-catenin binds actin fiber.[4] In the middle part of α-catenin, three modulation domains M1, M2, and M3 have native conformations which are mainly composed of α-helix bundles.[5]

In vitro experiment found that E-cadherin-β-catenin-α-catenin is the minimal protein complex to combine with actin fiber.[6] But the interaction between this protein complex and actin fiber is quite weak. Vinculin is another cross-linker protein which

*Corresponding author.

can bind α-catenin and actin fiber to reinforce the adhesion between α-catenin and actin fiber.[7] There is a binding site of vinculin on M1 domain of α-catenin, but the binding site is hidden inside the native conformation when α-catenin is free in cytosol. To recruit vinculin, its binding site on α-catenin must be accessible by vinculin, while stretching force can extend the conformation of α-catenin to expose this binding site of vinculin.[8,9] Besides vinculin, α-catenin also binds ZO1, afadin, formin, and spectrin.[2] Stretching force along α-catenin will affect the conformation and binding affinity of α-catenin with its binding partners to regulate biological processes orchestrated around adherens junction between cells.

α-catenin has been studied by single molecular manipulation methods of magnetic tweezer[8] and atomic force microscope.[10] It was found that at around 4.5 pN, M1 domain will unfold to expose binding site of vinculin, and binding of vinculin will block the refolding of M1 domain. With the force further increasing, M2 and M3 domains will unfold at force between 10 pN and 18 pN. When the force is relaxed, the unfolded domain will refold stepwisely.

Because M1 domain can unfold and refold in equilibrium at forces around 4.5 pN, its detailed force-dependent folding and unfolding dynamics has been obtained.[8] But the unfolding dynamics of M2 and M3 domain need more careful characterization. Here, we report the loading rate dependence of unfolding dynamics of α-catenin modulation domains, and more detailed information of unfolding and refolding dynamics is obtained.

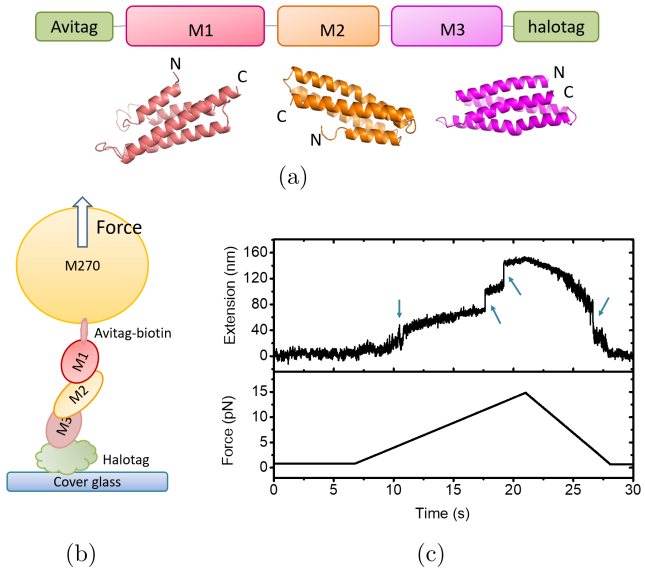

Fig. 1. Domain map of α-CM protein construct, schematic experimental setup, and typical experimental data. (a) Protein construct of α-CM protein is linked with avitag at N-terminus and halotag at C-terminus. Structures of modulation domains M1 (residues 277–393), M2 (residues 394–506), and M3 (residues 507–631) are adopted from crystal structure (PDB: 4IGG). (b) In magnetic tweezer experiment, α-CM protein is linked between cover glass surface and a paramagnetic bead M270 through which pulling force is applied to protein molecule. (c) During magnetic tweezer experiment, force is controlled by the instrument (bottom panel), and extension of protein is measured in real time by analysis of bead images (top panel). Originally, force is set as 0.78 pN and protein is at folded native conformation. Then force increases linearly to 15 pN with loading rate of 1 pN/s. After that, force decreases linearly to 0.78 pN with loading rate of -2 pN/s. The measured extension changes smoothly when there is no conformation transition, and jumps up suddenly when unfolding transition happens and jumps down suddenly when folding transition happens (indicated by arrows).

2. Materials and Methods

2.1. *Sample preparation*

The vector of α-catenin modulation domains (α-CM) contains an Avitag at the N-terminus, α-catenin modulation domains M1–M3, and a halotag followed with 6-Hisdine tag at the C-terminus (Fig. 1(a)). This vector and BirA vector were co-cloned into *E. coli* BL21 strain at the same time to express the protein. Then, we used Ni-NTA columns to purify the protein α-CM. Avitag of the purified protein was already ligated with biotin by BirA enzyme in bacteria. In the protein construct, halotag was used to attach protein to coverslip surface, and biotin was used to couple with stretavidin protein on surface of paramagnetic beads (Fig. 1(b)).

A home-made flow chamber was used to do single molecular manipulation experiment. Firstly, coverslips were cleaned by 5% detergent decon90 in sonicator for five minutes, then rinsed by ethanol and dried in oven at 80°C. Oxygen plasma cleaner was used to further clean the coverslips for 10 min. One percent solution of 3-aminopropyltriethoxysilane in methanol was used to silanize the cleaned coverslips for one hour. Then coverslips were rinsed in methanol and DI water, and dried in oven at 100°C for 30 min. Flow chamber was made by two pieces of coverslips and parafilm in between. Coverslips and parafilm stuck together by gentle heating on hot plate.

After the flow chamber was ready, 1% glutaraldehyde in DI water was added and incubated for one hour, then rinsed by DI water. Solution of polybead with amino surface was flowed into chamber to let the bead stuck on coverslip surface as reference bead in magnetic tweezer measurement. Halotag ligand chloroalkane with amine group in DI water was flowed into chamber and incubated for 1 h to attach on coverslip surface by reacting with aldehyde group. PBS buffer with 1% BSA, 0.0002% Tween-20 was flowed into the channel and incubated overnight to passivate the surface.

Halotag and biotin double-tagged α-CM protein were introduced to flow chamber, and incubated for 10 min. After washing away free protein in solution, streptavidin-coated paramagnetic beads (Dynal M-270 bead, Invitrogen) were introduced in the channel to form protein tethers (Fig. 1(b)). Then the chamber was put on magnetic tweezer to study its force response.

2.2. *Single molecular manipulation*

Home-made magnetic tweezers were built on an inverted optical microscope (IX73, Olympus). Hundred times oil-immersion objective was installed on a piezo objective actuator (PIFOC Nano focusing ZDrive, PI) to image the sample, and measure the extension of tethered protein. Two permanent magnetic rods with opposite polarization direction stuck together by magnetic force. Magnetic rods were put above the sample chamber, and the distance between magnets and sample was controlled by motorized stage (LS-110, PI) with stepper motors. Images of tethered bead and stuck bead were captured by CCD camera (Pike F032B). Power spectrum of bead image was used to compare the current image with images in a pre-stored image library at different focal planes, and bead location with spatial resolution better than 2 nm was realized by interpolation of the correlation values.[11,12]

Force as a function of the distance between magnets and sample $f(d)$ was calibrated using lambda phage DNA and the drag force in glycerol solution. By moving the magnets closer to the sample according to the inverse function of $f(d)$, the force was increased linearly with time. Similarly, the force can be decreased linearly with time by moving away the magnets from the sample.

3. Results

3.1. *Unfolding process at different loading rate*

Similar to previous magnetic tweezer experiment,[8] the protein tether was pulled by forces increasing from 0.78 pN to 15 pN with constant loading rate of 1 pN/s (Fig. 1(c)). At a force of 4.6 pN, the protein extension suddenly increases, which indicates the unfolding of one protein domain. The unfolded domain can refold and unfold again during this constant loading rate pulling process, and stay at the unfolded state when force is bigger than 5 pN. At 11.5 pN and 13.0 pN, two additional unfolding steps with step size of around 25 nm were observed. At a force of 15 pN, all domains in protein αCM were unfolded, then the force was decreased to 0.78 pN with a constant loading rate of -2 pN/s. At a force of 3.6 pN, the extension drops suddenly, indicating the start of the folding process of αCM. Further folding steps can be observed when the force decreases to around 1–2 pN. At the smallest force of 0.78 pN, the protein tether was held for one minute to make sure the protein folds to its original native state. Then the same force-increasing and force-decreasing cycles were applied to obtain enough statistical data points.

In the previous paper,[8] the first unfolding step was identified as the unfolding of M1 domains with vinculin binding site by a study of the mutant protein L344P αCM. Equilibrium folding and unfolding dynamics at constant forces were studied in detail to get the dynamic parameters of M1 domain. The results showed that the transition state of M1 is in the middle of the native state and unfolded state: the distance between transition state and native state is $x_u \sim 8.2$ nm, and the distance between transition state and unfolded state is $x_f \sim 7.4$ nm. However, the dynamic parameters of M2 and M3 domains are still unknown. As the native conformations of these modulation domains share the same type of conformation composed of four α-helix, the transition distances of x_u and x_f might have similar values.

Here, the unfolding dynamics of M2 and M3 domains are studied by applying different loading rates. For a single αCM protein tether, multiple force cycles were applied. In different force cycles, the loading rates of the force increase process were changed from 0.1 pN/s to 4 pN/s (Fig. 2), and the unfolding forces of M2 and M3 domains were recorded.

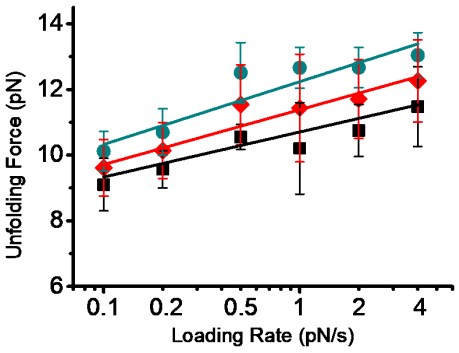

Fig. 2. The loading rate-dependent unfolding forces of α-CM M2 and M3 domains. Black squares show the mean unfolding force of the first unfolding step, while cyan circles show the mean unfolding force of the second unfolding step. Red diamonds give the average unfolding force of these two domains. Each data point is obtained from average of at least 24 measurements. The error bar denotes the standard deviation of unfolding force at each loading rate. The solid lines denote linear fitting results.

We suppose that the force-dependent unfolding rates of M2 and M3 domains $k_u(f)$ follow Bell's model in the unfolding force range from 8 to 14 pN[13]:

$$k_u(f) = k_u^0 \exp(fx_u/k_BT), \tag{1}$$

where k_u^0 is the unfolding rate at zero force, x_u is the unfolding distance, k_B is Boltzmann constant, and T is the absolute temperature. From the loading-rate-dependent unfolding force and its distribution, theoretical method can be used to get the dynamic parameters.[14–16] With constant loading rate r, i.e., $f = rt$, the most probable unfolding force F_{max} is given by

$$F_{max} = \frac{k_BT}{x_u} \ln \frac{rx_u}{k_u^0 k_BT}. \tag{2}$$

Theoretically, the unfolding force distribution is not symmetric. Because of the limited data point at each loading rate, the most probable unfolding force F_{max} cannot be obtained accurately. Therefore, we use the average unfolding force as an approximation of F_{max}. From the slope of mean unfolding force of M2 and M3 domains as a function of $\ln r$ (red line in Fig. 2), x_u is estimated to be ~ 5.6 nm. Because the step sizes of M2 and M3 domains are similar, we do not know which domain unfolds firstly. The slope of the first unfolding force as a function of $\ln r$ (black line in Fig. 2) gives $x_u \sim 6.9$ nm, while that of the second unfolding force gives $x_u \sim 4.9$ nm. Though the unfolding distances of M2 and M3 domains are smaller than that of M1 domain (8.2 nm), they are still much longer than the typical unfolding distance of proteins subjected to shearing force like titin I27 and GB1.[17,18]

3.2. *Intermediate unfolding state identification*

At slow loading rate ≤ 0.2 pN/s, we can observe an additional state with extension ~ 5 nm longer than the state with just M1 domain unfolded in the time trace right before the unfolding steps of M2/M3 domains (Fig. 3). This additional state is supposed to be an unfolding intermediate state. The lifetime of this intermediate state is usually less than 0.2 s. This unfolding intermediate state was ignored before at big loading rate, which is consistent with the fact that the probability to observe this intermediate state decreases with increasing loading rate. Sometimes, the full unfolding step occurs from this unfolding intermediate state (Fig. 3(a)), while sometimes this intermediate state folds back to native state before the full unfolding step (Fig. 3(b)). Therefore, this intermediated state can be an on-pathway unfolding intermediate state or off-pathway unfolding intermediate state.

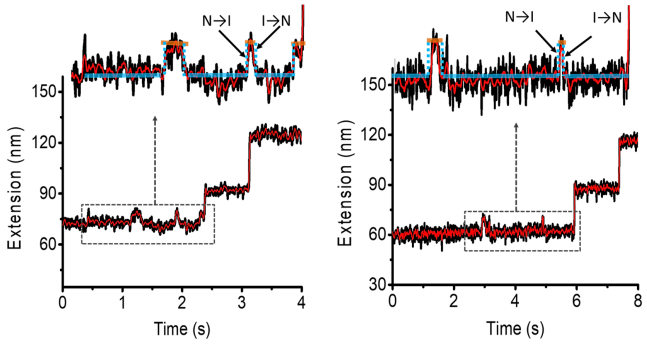

Fig. 3. Intermediate unfolding state during force-increasing process with slow loading rate of 0.2 pN/s. Before the first unfolding step of M2 and M3 domains, extension of protein jumps up by step of ~ 5 nm and jumps down to original value for several times. Horizontal lines indicate the native conformation (cyan color) and unfolding intermediate state (brown color), and arrows and vertical dotted lines indicate the transition from native conformation to intermediate state (N $\rightarrow$ I) and inverse transition (I $\rightarrow$ N). (a) Unfolding step of M2 and M3 domains occurs from this intermediate state. (b) Unfolding step of M2 and M3 domains occurs from the native state of M2 and M3 domains.

3.3. *Force-dependent folding process*

Fully unfolded conformation at big force is an extended polypeptide. With decreasing force, fully unfolded α-CM can fold to its native state, which has been verified by the repeatable multicycle protein pulling process. When stretching force applied on fully unfolded α-CM drops to the critical force of ~ 4.7 pN, the conformation fluctuation of M1 domain cannot be observed, which indicates that the folding of M1 domain is dependent on the conformation of M2/M3 domains. During the force-decreasing process with loading rate of -2 pN/s, α-CM folds to its native state by two main steps and further conforms to the searching process at low force. The first main folding step occurs at a force around 3.7 pN with standard deviation of 0.3 pN (Fig. 4(a)). Though we do not know which part of α-CM folds in this first folding step, some useful information of the folding dynamics can be estimated. We suppose folding rate $k_f(f)$ of this first folding step follows Bell's model:

$$k_f(f) = k_f^0 \exp(-f x_f / k_B T), \tag{3}$$

where x_f is the distance between unfolded peptide and the folding transition state at forces around 3.7 pN. By using the probability optimization method,[16] we estimate the parameter $x_f \sim 13$ nm by optimizing the combined probability of all time traces.

When we zoomed in the time trace, we found more detailed information about this folding step. Though it usually takes less than 0.1 s, the folding processes are not all identical. They can be classified into three typical types of processes: one with a single big step of more than 30 nm, one with two consecutive small steps, and one with continuous linear process (Fig. 4(b)). Therefore, the folding can go through different pathways. The pathway with a single big step indicates that two domains can fold at the same time with high cooperativity.

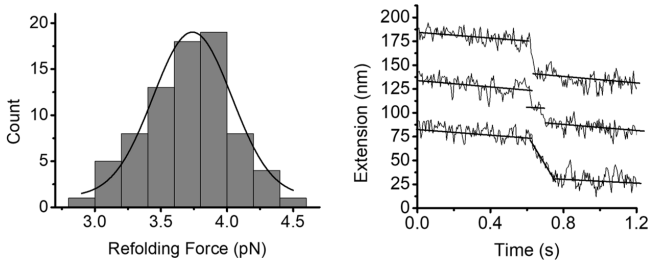

(a) (b)

Fig. 4. The first folding step of α-CM molecule during force-decreasing process at constant loading rate of -2 pN/s. (a) Histogram of refolding force of this first folding step. The red line represents Gaussian fitting curve. The data are from 77 independent unfolding events. (b) Three typical folding steps at ~ 3.6 pN. Curves are shifted vertically for clarity. Top one shows a single step of ~ 34 nm. Middle one shows two consecutive steps of ~ 17 nm. Bottom one shows a continuous linear folding process with slop.

4. Conclusion and Discussion

As a key protein in the cell–cell coherense junction, α-catenin works not only as a crosslinker to connect cadherine/β-catenin with F-actin cytoskeleton, but also as a force sensor. The force-induced conformation change and unfolding of its modulation domains will absorb the work done by internal and external forces, and α-catenin works as a force buffer similar to tilin.[19] At the same time, the force-induced conformation change also exposes the binding site to recruit vinculin to reinforce the connection between α-catenin and actin fiber.

Modulation domains M1–M3 of α-catenin have native conformation composed of α-helix bundles. Each of these three modulation domains has four α-helixes. Usually, the topological conformation, especially the force pulling geometry, plays an important role in the mechanical stability of proteins. Modulation domains of α-catenin unfold at forces less than 20 pN. Compared with immunoglobulin domain I27 of titin which is composed of seven β-strands, α-catenin is much less mechanical stable. As the structure and pulling geometry of each α-catenin modulation domain are similar, different unfolding forces between M1 and M2/M3 domains should come from detailed interaction in each domain.

From both previous equilibrium measurement of M1 domain and our measurement of the loading rate-dependent unfolding forces of M2 and M3 domains, the unfolding distance, which is defined as the extension difference between unfolding transition state and native state, is around 5–8 nm. It indicates that the extension of unfolding transition state is much longer than the distance between N-terminus and C-terminus of each modulation domain in the native state. Please note that the unfolding distance of titin I27 is only 0.25–0.3 nm as measured by atomic force microscope at a force greater than 100 pN,[17,20] and around 0.57 nm at a force between 50 and 100 pN[21] as measurement by

magnetic tweezers. At forces smaller than 20 pN, unfolding distance of I27 is negative to give catch bond behavior.[21] Long unfolding distance x_u of α-catenin makes its unfolding very sensitive to stretching force. As a force sensor, the sensitivity to force is critical to its biological function.

When all three domains are unfolded, equilibrium folding/unfolding dynamic process of M1 domain at 4–5 pN is not detected, which indicates the stability and folding dynamics of M1 domain depends on the conformation of M2 and M3 domains. During the force-decreasing process, the first folding step has a step size of more than 30 nm, which indicates that the folding of M1–M3 domains is a cooperative process. With decreasing force, the folding process of α-CM domains can go through different pathways.

Conflict of Interest

The authors declare no conflict of interest.

Acknowledgments

We are grateful to Jie Yan from National University of Singapore and René-Marc Mège from Université Paris Diderot for the kind gift of α-catenin vector. This research was supported by the National Nature Science Foundation of China (Grant Nos. 11474237 and 11574310), and the 111 Project (Grant No. B16029).

References

1. U. Cavallaro, E. Dejana, "Adhesion molecule signalling: Not always a sticky business," *Nat. Rev. Mol. Cell Biol.* **12**, 189–197 (2011).
2. A. Kobielak, E. Fuchs, "Alpha-catenin: At the junction of intercellular adhesion and actin dynamics," *Nat. Rev. Mol. Cell Biol.* **5**, 614–625 (2004).
3. G. A. Gomez, R. W. McLachlan, A. S. Yap, "Productive tension: Force-sensing and homeostasis of cell–cell junctions," *Trends Cell Biol.* **21**, 499–505 (2011).
4. T. Lecuit, "Alpha-catenin mechanosensing for adherens junctions," *Nat. Cell Biol.* **12**, 522–524 (2010).
5. E. S. Rangarajan, T. Izard, "Dimer asymmetry defines α-catenin interactions," *Nat. Struct. Mol. Biol.* **20**, 188–193 (2013).
6. C. D. Buckley, J. Tan, K. L. Anderson, D. Hanein, N. Volkmann, W. I. Weis, W. J. Nelson, A. R. Dunn, "The minimal cadherin-catenin complex binds to actin filaments under force," *Science* **346**, 1254211–1254218 (2014).
7. X. Peng, E. S. Nelson, J. L. Maiers, K. A. DeMali, "New insights into vinculin function and regulation," *Int. Rev. Cell Mol. Biol.* **287**, 191–231 (2011).
8. M. Yao, W. Qiu, R. Liu, A. K. Efremov, P. Cong, R. Seddiki, M. Payre, C. T. Lim, B. Ladoux, R. M. Mege, J. Yan, "Force-dependent conformational switch of α-catenin controls vinculin binding," *Nat. Commun.* **5**, 4525–4535 (2014).
9. M. Yao, B. T. Goult, H. Chen, P. Cong, M. P. Sheetz, J. Yan, "Mechanical activation of vinculin binding to talin locks talin in an unfolded conformation," *Sci. Rep.* **4**, 4610–4616 (2014).
10. K. Maki, S. W. Han, Y. Hirano, S. Yonemura, T. Hakoshima, T. Adachi, "Mechano-adaptive sensory mechanism of α-catenin under tension," *Sci. Rep.* **6**, 24878–24896 (2016).
11. H. Chen, H. Fu, X. Zhu, P. Cong, F. Nakamura, J. Yan, "Improved high-force magnetic tweezers for stretching and refolding of proteins and short DNA," *Biophys. J.* **100**, 517–523 (2011).
12. H. Chen, G. Yuan, R. S. Winardhi, M. Yao, I. Popa, J. M. Fernandez, J. Yan, "Dynamics of equilibrium folding and unfolding transitions of titin immunoglobulin domain under constant forces," *J. Am. Chem. Soc.* **137**, 3540–3546 (2015).
13. G. I. Bell, "Models for the specific adhesion of cells to cells," *Science* **200**, 618–627 (1978).
14. T. Strunz, K. Oroszlan, R. Schafer, H. J. Guntherodt, "Dynamic force spectroscopy of single DNA molecules," *Proc. Natl. Acad. Sci. U.S.A.* **96**, 11277–11282 (1999).
15. T. A. Sulchek, R. W. Friddle, K. Langry, E. Y. Lau, H. Albrecht, T. V. Ratto, S. J. DeNardo, M. E. Colvin, A. Noy, "Dynamic force spectroscopy of parallel individual Mucin1-antibody bonds," *Proc. Natl. Acad. Sci. U.S.A.* **102**, 16638–16643 (2005).
16. W. Zhai, G. Yuan, C. Liu, H. Chen, "Improved data analysis method of single-molecule experiments based on probability optimization," *Chin. Phys. B* **27**, 18703–18708 (2018).
17. M. Carrion-Vazquez, A. F. Oberhauser, S. B. Fowler, P. E. Marszalek, S. E. Broedel, J. Clarke, J. M. Fernandez, "Mechanical and chemical unfolding of a single protein: A comparison," *Proc. Natl. Acad. Sci. U.S.A.* **96**, 3694–3699 (1999).
18. Y. Cao, C. Lam, M. Wang, H. Li, "Nonmechanical protein can have significant mechanical stability," *Angew. Chem. Int. Ed. Engl.* **45**, 642–645 (2006).
19. M. Yao, B. T. Goult, B. Klapholz, X. Hu, C. P. Toseland, Y. Guo, P. Cong, M. P. Sheetz, J. Yan,

"The mechanical response of talin," *Nat. Commun.* **7**, 11966–11976 (2016).

20. P. M. Williams, S. B. Fowler, R. B. Best, J. L. Toca-Herrera, K. A. Scott, A. Steward, J. Clarke, "Hidden complexity in the mechanical properties of titin," *Nature* **422**, 446–449 (2003).
21. G. Yuan, S. Le, M. Yao, H. Qian, X. Zhou, J. Yan, H. Chen, "Elasticity of the transition state leading to an unexpected mechanical stabilization of titin immunoglobulin domains," *Angew. Chem. Int. Ed. Engl.* **56**, 5490–5493 (2017).